A Co-Delivery System Based On Paclitaxel Grafted mPEG-b-PLG Loaded with Doxorubicin: Preparation, In Vitro and In Vivo Evaluation.

7 AUTHORS, INCLUDING:

Shixian Lv
Chinese Academy of Sciences
18 PUBLICATIONS **258** CITATIONS

SEE PROFILE

Zhaohui Tang
Changchun Institute of Applied Chemistry …
74 PUBLICATIONS **1,910** CITATIONS

SEE PROFILE

Yan Yang
Jilin University
66 PUBLICATIONS **628** CITATIONS

SEE PROFILE

A co-delivery system based on paclitaxel grafted mPEG-b-PLG loaded with doxorubicin: Preparation, in vitro and in vivo evaluation

Qian Li [a,b], Shixian Lv [a,d,1], Zhaohui Tang [a,*], Muhua Liu [b,**], Dawei Zhang [a], Yan Yang [c], Xuesi Chen [a]

[a] Key Laboratory of Polymer Ecomaterials, Changchun Institute of Applied Chemistry, Chinese Academy of Sciences, Changchun 130022, PR China
[b] Engineering College, Jiangxi Agriculture University, Nanchang 330045, PR China
[c] Key Laboratory for Molecular Enzymology and Engineering of Ministry of Education, Jilin University, Changchun 130012, PR China
[d] University of Chinese Academy of Sciences, Beijing 100049, PR China

A B S T R A C T

Herein, we develop a co-delivery system of paclitaxel (PTX) and doxorubicin hydrochloride (DOX·HCl) based on methoxypoly(ethylene glycol)-block-poly(L-glutamic acid) (mPEG-b-PLG) for cancer treatment. PTX was grafted to the mPEG-b-PLG by esterification to give mPEG-b-PLG-g-PTX. DOX·HCl was encapsulated via electrostatic interaction and hydrophobic stack between the DOX·HCl and mPEG-b-PLG-g-PTX in aqueous solution. The release rate of DOX·HCl from the drug-loaded nanoparticles (mPEG-b-PLG-g-PTX-DOX) was slow at blood pH (pH 7.4), but obviously increased at endosome pH (pH 5.4). The mPEG-b-PLG-g-PTX-DOX exhibited slight synergistic effect in inhibition of proliferation of A549 and MCF-7 human cancer cells. For in vivo treatment of xenograft human breast tumor (MCF-7), the mPEG-b-PLG-g-PTX-DOX nanoparticles exhibited remarkable tumor inhibition effect with a 95.5% tumor-suppression-rate which was significantly higher than those of related single anticancer agents such as free DOX·HCl and mPEG-b-PLG-g-PTX. These results indicated that the mPEG-b-PLG-g-PTX-DOX would have great potential in cancer therapy.

© 2014 Elsevier B.V. All rights reserved.

1. Introduction

Cancer is a leading cause of death worldwide and chemotherapy is the most commonly used treatment in cancer therapy (Siegel et al., 2013). However, the therapeutic effect of chemotherapy is still limited. Severe side effects often occur due to non-specific drug distribution (Kieler-Ferguson et al., 2013). To overcome these problems, nanocarriers with a variety of architectures including polymer-drug conjugates (Chen et al., 2012; Pan et al., 2013), micelles (Lei et al., 2013; Xu et al., 2007; Zhong et al., 2013), nanogels (Li et al., 2014), liposomes (Xiang et al., 2013), and nanospheres (Shen et al., 2014), had been developed for antitumor drug delivery (Duncan, 2006; Park et al., 2008). These nano-medicines can deliver more drugs to solid tumors by the enhanced permeability and retention (EPR) effect and have improved pharmacokinetics and biodistribution profiles (Huynh et al., 2009), so that reduced side-effects and enhanced antitumor efficacy were obtained (Deng et al., 2012; Wang et al., 2007).

* Corresponding author. Tel.: +86 431 85262116; fax: +86 431 85262116.
** Corresponding author. Tel.: +86 791 83813260; fax: +86 791 83813260.
E-mail addresses: ztang@ciac.ac.cn (Z. Tang), suikelmh@sina.com (M. Liu).
[1] These authors contributed equally to this work.

Anticancer drugs can be loaded into nanocarriers through electrostatic, hydrophobic interactions, or covalent bonding (Li et al., 2013a; Liu et al., 2012; Song et al., 2012b). To get better therapeutic effects and to reduce the multi-drug resistance, the combination chemotherapy with two or more drugs was often used in the clinical treatment (Boulikas and Vougiouka, 2004), but in most of the reported delivery systems just one anticancer agent was applied (Blanco et al., 2011; Li et al., 2012; Park et al., 2008; Song et al., 2012c). Therefore, it is deserved to explore co-delivery system which can deliver two or more drugs within one vehicle (Lee et al., 2009; Xiao et al., 2012).

Among many of the nanocarriers, the polypeptide-based polymers have attracted great attention due to their good biocompatibility and biodegradability (Choe et al., 2012; Deming, 2007). Variety of drug delivery systems using the polypeptide-based polymers as carriers have entered the stage of clinical evaluation (Matsumura, 2008). For example, a phase II study of SN-38-conjugated poly(ethylene glycol)-*block*-poly(glutamic acid) (NK012) against advanced metastatic triple negative breast cancer is now ongoing (Greenberg and Rugo, 2010). Phase III studies of paclitaxel poliglumex (CT2103, PPX), paclitaxel incorporated micelle of poly(ethylene glycol)-*block*-poly(aspartate) with 4-phenyl-1-butanol modification (NK105), and cisplatin incorporated micelles of poly(ethylene glycol)-*block*-poly(glutamic acid) (NC-6004) are also underway (Reddy and Bazile, 2013; Zhang et al., 2013).

Doxorubicin hydrochloride (DOX·HCl) is an anthracycline antibiotic that works by intercalating DNA. Its side effects, such as the dose-dependent cardiotoxicity, myelosuppression, nephrotoxicity, and development of multidrug resistance, limit the use of the drug (Weiss, 1992). Paclitaxel (PTX) is a representative microtubule-stabilizing chemotherapy drug, its hydrophobicity and serious side effects limit its use in clinical practice (Rowinsky et al., 1993). The combination of DOX·HCl and PTX was found to be highly effective in the treatment of advanced breast cancer, but was accompanied by the dose-limiting toxic effects of neutropenia, neuropathy, and cardiotoxicity (Gehl et al., 1996).

For the benefit of patients, it is necessary to address the limitations of DOX·HCl and PTX so that the anticancer drugs can work more efficiently. In order to develop the drug delivery system containing the advantages of combination chemotherapy that is widely used in clinical practice, we determine to make a co-delivery system that can deliver both DOX·HCl and PTX with one vehicle. Poly(L-glutamic acid) has shown its potential as nano-vehicles of PTX and DOX·HCl. For example, poly(L-glutamic acid)-paclitaxel conjugate has entered phase III clinical trials (Langer et al., 2008). We have reported DOX·HCl-loaded nanoparticles using methoxypoly(ethylene glycol)-*b*-poly(L-glutamic acid) or methoxy poly(ethylene glycol)-*b*-poly(L-glutamic acid-*co*-L-phenylalanine) as nanovehicle. These nanomedicines exhibited enhanced therapeutic efficacy and reduced side effects in nude mice bearing A549 lung cancer xenograft, as compared with free DOX·HCl (Li et al., 2013b; Lv et al., 2013).

In this work, a conjugate of mPEG-*b*-PLG and PTX (mPEG-*b*-PLG-*g*-PTX) was prepared and used for the systhesis of DOX·HCl-loaded mPEG-*b*-PLG-*g*-PTX nanoparticles (mPEG-*b*-PLG-*g*-PTX-DOX). The co-delivery system of mPEG-*b*-PLG-*g*-PTX-DOX was assessed for physicochemical properties, release profile, cellular uptake, *in vitro* cytotoxicity, and *in vivo* antitumor efficacy.

2. Experimental

2.1. Materials

Poly(ethylene glycol) monomethyl ether (mPEG, M_n = 5000) was purchased from Aldrich. The amino group terminated poly(ethylene glycol) monomethyl ether (mPEG-NH$_2$) and γ-benzyl-L-glutamate-

N-carboxyanhydride (BLG-NCA) were synthesized as reported earlier (Song et al., 2012a). Doxorubicin hydrochloride and paclitaxel were purchased from Beijing Huafeng United Technology Corporation, China. Fluorescein isothiocyanate (FITC) was bought from Aladdin Company, China. *N,N*′-Dimethylformamide (DMF) was stored over calcium hydride (CaH$_2$) and purified by vacuum distillation before use. 3-(4,5-Dimethyl-thiazol-2-yl)-2,5-diphenyl tetrazolium bromide (MTT) and 4′,6-diamidino-2-phenylindole dihydrochloride (DAPI) were purchased from Sigma and used as received. Clear polystyrene tissue culture treated 6-well and 96-well plates were obtained from Corning Costar. Purified deionized water was prepared by the Milli-Q plus system (Millipore Co., Billerica, MA, USA). All other reagents and solvents were purchased from Sinopharm Chemical Reagent Co., Ltd., China and used as received.

2.2. Characterization

^{1}H NMR spectra were recorded on a Bruker AV 400 NMR spectrometer in trifluoroacetic acid-d (CF$_3$COOD), except the mPEG-*b*-PLG-*g*-PTX in which a mixture of CF$_3$COOD and dimethylsulfoxide-D6 (DMSO-d6) was used as solvent. Number-, weight-average molecular weights (M_n, M_w) and weight distribution (M_w/M_n) of mPEG-*b*-PBLG were measured by gel permeation chromatography (GPC), a series of linear Tskgel Super columns (AW3000 and AW5000), Water 515HPLC pump and OPTILAB DSP Interferometric Refractometer (Wyatt Technology) were the main hardwares of the instrument. The chromatographic condition was as follows: DMF containing 0.01 M lithium bromide (LiBr) was used as eluent at a flow rate of 1.0 mL min^{-1} under 50 °C, monodispersed polystyrene standards were used to generate the calibration curve, particle size and zeta potentials (ζ-potential) measurement of nanoparticles (NPs) was carried out on a Zeta Potential/BI-90Plus particle size analyzer (Brookhaven, USA) at 25 °C, and confocal laser scanning microscopy (CLSM) observations were carried out using Carl Zeiss LSM 700.

2.3. Synthesis of mPEG-b-PLG diblock copolymer

mPEG-*b*-PLG diblock copolymer was synthesized as our previous work (Li et al., 2013b; Song et al., 2012a). To a dried and nitrogen-purged ampule, BLG-NCA monomer (6.588 g, 25.0 mmol) and mPEG-NH$_2$ (5.0 g, 1.0 mmol) were added. Dry DMF (110 mL) was then injected by a syringe. After stirring at 25 °C for 3 days, the reaction mixture was precipitated into excess ether to give methoxy poly(ethylene glycol)-*b*-poly(γ-benzyl-l-glutamate) (mPEG-*b*-PBLG) block copolymers. Subsequently, 5.145 g of mPEG-*b*-PBLG was dissolved in 50 mL of dichloroacetic acid at room temperature in a flask. After 11 mL of HBr/acetic acid (33 wt%) was added, the solution was stirred at 30 °C for 1 h and then precipitated into excessive ether. After dried under vacuum for 24 h, the precipitate was dialyzed against distilled water and freeze-dried, yielding mPEG-*b*-PLG as a white solid. ^{1}H NMR of mPEG-*b*-PLG in CF$_3$COOD: δ 4.80 ppm (—COCH<), 3.87 ppm (—CH$_2$CH$_2$O—), 2.63 ppm (—CH$_2$CO—), 2.28 and 2.13 ppm (>CHCH$_2$CH$_2$—).

2.4. Synthesis of mPEG-b-PLG-g-PTX

mPEG-*b*-PLG-*g*-PTX was synthesized through a condensation reaction between mPEG-*b*-PLG and PTX using diisopropylcarbodiimide (DIC) as condensing agent and 4-dimethylaminopyridine (DMAP) as catalytic agent. The detail process was as follows: After mPEG-*b*-PLG (2.056 g, 0.25 mmol), PTX (0.707 g, 0.875 mmol), and DMAP (0.0765 g, 0.657 mmol) were weighted into a flame-dry flask and vacuumized for 12 h, dry DMF (27 mL) was added in to the dissolved mixture. DIC (0.661 g, 5.25 mmol) was then added. After the reaction was carried out under stirring at 25 °C for 24 h, the

reaction mixture was precipitated into excess amount of cold ether 3 times to get mPEG-b-PLG-g-PTX crude product. The crude product was then dissolved in DMF and dialyzed against DMF to remove free PTX. Purified mPEG-b-PLG-g-PTX was obtained as a white solid by dialysis against distilled water and subsequent lyophilization. ^{1}H NMR of mPEG-b-PLG-g-PTX in CF$_3$COOD/DMSO-d6: δ 8.31–7.15 ppm (aromatic protons from PTX), 3.62 ppm (—CH$_2$CH$_2$O—from mPEG), other signals are overlapped and broad.

2.5. Preparation of mPEG-b-PLG-g-PTX-DOX nanoparticles

mPEG-b-PLG-g-PTX (300 mg) was weighted and dissolved in deionized water (20 mL). The pH value of the solution was adjusted to 7–8 with 1 mol/L sodium hydroxide solution. DOX·HCl (28.0 mg) was dissolved in deionized water (5 mL) and added into the mPEG-b-PLG-g-PTX solution. The obtained mixture was vigorously stirred in the dark overnight. Free DOX·HCl was removed by dialysis (MWCO 3500) against deionized water for 24 h (The dialysis medium was changed five times) and followed by lyophilization in the dark. To figure out the loading content and loading efficiency of DOX·HCl, lyophilized mPEG-b-PLG-g-PTX-DOX nanoparticles were dissolved in N,N'-dimethylformamide (DMF) and measured by a UV–vis spectrometer at 480 nm. Drug loading content (DLC) and drug loading efficiency (DLE) were calculated according to the following formulas:

$$DLC(wt\%) = \left(\frac{\text{weight of loaded drug}}{\text{weight of drug} - \text{loaded NPs}} \right) \times 100\%$$

$$DLE(wt\%) = \left(\frac{\text{weight of loaded drug}}{\text{weight of feeding drug}} \right) \times 100\%$$

FITC labeled mPEG-b-PLG-g-PTX-DOX was prepared as follows: mPEG-b-PLG-g-PTX lyophilized powder (100.0 mg) and FITC (5.0 mg) were dissolved in DMF (6.0 mL). After being stirred overnight at room temperature, the FITC labeled mPEG-b-PLG-g-PTX was purified by dialysis against deionized water for 96 h. A light yellow powder was obtained after lyophilization. DOX·HCl was loaded into FITC labeled mPEG-b-PLG-g-PTX according to the method utilized for the mPEG-b-PLG-g-PTX-DOX nanoparticles.

2.6. In vitro release of DOX

To investigate the release of DOX from the mPEG-b-PLG-g-PTX-DOX nanoparticles, the weighted freeze-dried nanoparticles were resuspended in 5 mL of phosphate buffered saline (PBS) and transferred into a dialysis bag (MWCO 3500 Da). The dialysis bag was immersed into 45.0 mL of PBS (pH 5.4, 6.8 or 7.4) with constant shaking (100 rpm) at 37 °C. At selected time intervals, 3.0 mL of the solution outside the dialysis bag was removed for analysis and replaced by the same volume of fresh PBS. The concentration of DOX released in the dialysate was determined using UV–vis spectrometer at 480 nm.

2.7. Cell culture

Human breast cancer cells (MCF-7) and the human lung carcinoma (A549) cells were cultured at 37 °C in a 5% CO$_2$ atmosphere. Dulbecco's modified Eagle's medium (DMEM, Gibco) supplemented with 10% fetal bovine serum, penicillin (50 U mL^{-1}), and streptomycin (50 U mL^{-1}) was used as culture medium.

2.8. Confocal laser scanning microscopy (CLSM) observation

To investigate the cellular uptake and intracellular release behavior of mPEG-b-PLG-g-PTX-DOX nanoparticles, CLSM observation toward MCF-7cells was performed. The cells were seeded on coverslips in 6-well plates which included 2 mL of DMEM with a density of 1×10^5 cells per well and cultured for 24 h. Then experimental samples were added. The concentration of free DOX·HCl and FITC labeled mPEG-b-PLG-g-PTX-DOX was 5 µg/mL on the basis of DOX·HCl. The concentration of FITC labeled mPEG-b-PLG-g-PTX was 16 µg/mL on the basis of PTX. After 1 or 3 h incubation, the cells were washed with PBS (pH 7.4) and fixed with 4% paraformaldehyde for 10 min at 37 °C. The cell nucleus were stained with 0.1% DAPI for 10 min in the dark. The spare DAPI was washed with PBS (pH 7.4). The treated cells were visualized under a laser scanning confocal microscope (Carl Zeiss LSM 700).

2.9. Cytotoxicity assay

The cytotoxicities of mPEG-b-PLG-g-PTX and mPEG-b-PLG-g-PTX-DOX nanoparticles against MCF-7cells and A549cells were evaluated by MTT assay. The cells were seeded in 96-well plates (6×10^3 cells per well) with 100 µL of DMEM medium in every well and incubated at 37 °C in a 5% CO$_2$ atmosphere for 24 h. The old culture mediums were replaced with 200 µL of fresh mediums containing free DOX·HCl, mPEG-b-PLG-g-PTX or mPEG-b-PLG-g-PTX-DOX. The cells were subjected to MTT assay after being incubated for another 48 h or 72 h. The absorbency of the solution was measured with a Bio-Rad 680 microplate reader at 490 nm. The relative cell viability was calculated by comparing the absorption value of experimental wells at 490 nm with control wells that contained cell culture medium only. Data are presented as means ± standard deviation ($n = 3$).

The synergistic, additive, or antagonistic cytotoxic effects were evaluated from combination index (CI) analysis based on the Chou and Talalay's method (Chou, 2006; Song et al., 2014) using the following equation:

$$CI_x = \frac{(D)_1}{(D_x)_1} + \frac{(D)_2}{(D_x)_2}$$

$(D_x)_1$ and $(D_x)_2$ represent the IC$_x$ value of drug 1 alone and drug 2 alone, respectively. $(D)_1$ and $(D)_2$ represent the concentration of drug 1 and drug 2 in the combination system at the IC$_x$ value. Values of CI > 1 represent antagonism, CI = 1 represent additive and CI < 1 represent synergism.

2.10. In vivo antitumor efficiency

Six-weeks-old female Balb/C nude mice obtained from Beijing HFK bioscience Co., Ltd. were used as experimental animals. According to the guidelines described in the Guide for the Care and Use of Laboratory Animals, all experimental animals received well care. The entire procedures of these experiments were approved by the Animal Care and Use Committee of Jilin University. Orthotopic tumor model was built through subcutaneous injecting MCF-7cells (2×10^6) in the right mammary fat pad of each mouse. When the tumor volume was approximately 25–50 mm^3, the mice were divided into 4 groups, then treated with PBS, free DOX·HCl (Dosage: 5 mg kg^{-1}), mPEG-b-PLG-g-PTX (Dosage: 16 mg kg^{-1} on a PTX basis), mPEG-b-PLG-g-PTX-DOX (Dosage: 5 mg kg^{-1} on a DOX·HCl basis, 16 mg kg^{-1} on a PTX basis) by tail intravenous injection on days 0, 4, 8, and 12. The tumor sizes were measured every two days. The tumor volume (mm^3) was calculated using $V = ab^2/2$, in this formula a and b standed for the longest and shortest diameter of the tumors, respectively. Tumor suppression rate (TSR%) = $[(V_c - V_x)/V_c] \times 100\%$, here, V_c represented the tumor volume of control group, while V_x represented the tumor volume of treatment group.
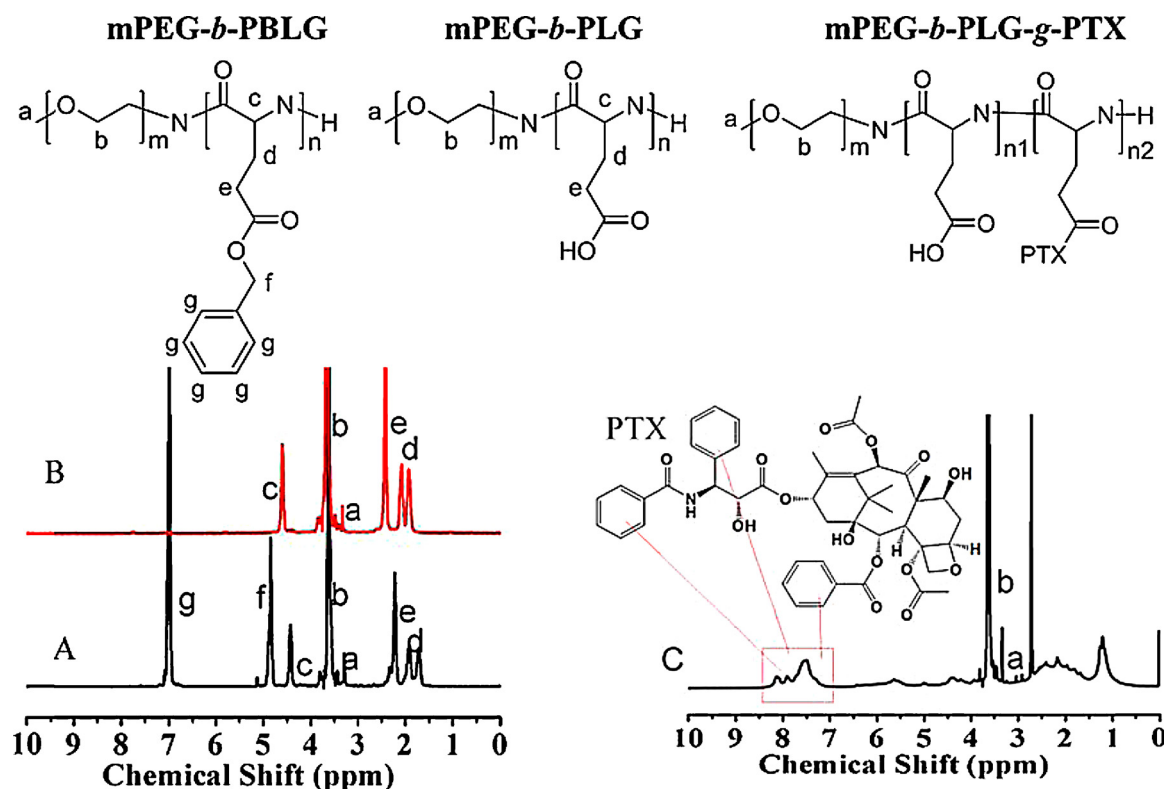
Fig. 1. ^{1}H NMR spectra of mPEG-*b*-PBLG (A), mPEG-*b*-PLG (B) in CF$_3$COOD, and mPEG-*b*-PLG-*g*-PTX (C) in the mixture solvent of CF$_3$COOD and DMSO-d6 (1:1, v/v).

3. Results and discussion

3.1. Preparation and characterization of mPEG-b-PLG, mPEG-b-PLG-g-PTX and mPEG-b-PLG-g-PTX-DOX

mPEG-*b*-PLG was prepared *via* a two-step method. Firstly, mPEG-*b*-poly(γ-benzyl-ʟ-glutamate) (mPEG-*b*-PBLG) diblock copolymer was synthesized by a ring-opening polymerization of BLG-NCA using mPEG-NH$_2$ as the initiator. Secondly, mPEG-*b*-PLG was generated by the deprotection of γ-benzyl from mPEG-*b*-PBLG in HBr/acetic acid (33 wt%). The ^{1}H NMR spectra of mPEG-*b*-PBLG and mPEG-*b*-PLG in CF$_3$COOD were shown in Fig. 1A and B with the relevant peaks labeled. The peaks *f* and *g* in the spectrum of mPEG-*b*-PBLG disappeared in that of mPEG-*b*-PLG, indicating the complete deprotection of the γ-benzyl groups (C$_6$H$_5$—, 5H and C$_6$H$_5$CH$_2$—, 2H). Through calculating the ratio of integration at peak *e*

(—COCH$_2$—, 2H, PBLG or PLG block) and peak *b* (—CH$_2$CH$_2$O—, 4H, PEG block), the polymerization degree of BLG and LG blocks were both determined to be 25, which indicated the deprotection reaction did not break the poly(ʟ-glutamic acid) backbones. Only an unimodal and symmetric peak was observed from the GPC curve of the mPEG-*b*-PBLG copolymer with the molecular weight distribution of 1.46. This revealed that ʟ-glutamic acid monopolymer and mPEG were not existed in the product. mPEG-*b*-PLG was prepared successfully.

mPEG-*b*-PLG-*g*-PTX was synthesized by the condensation reaction of mPEG-*b*-PLG with PTX using DIC as condensing agent and DMAP as catalytic agent. The ^{1}H NMR spectrum of mPEG-*b*-PLG-*g*-PTX in the mixture solvent of CF$_3$COOD and DMSO-d6 was shown in Fig. 1C. The appearance of peaks (benzene rings protons) in the range of δ 7.15–8.31 ppm indicated that PTX was successfully grafted on mPEG-*b*-PLG. By comparing the ratio of integration of all peaks in the range of δ 7.15–8.31 ppm (15H, benzene rings protons
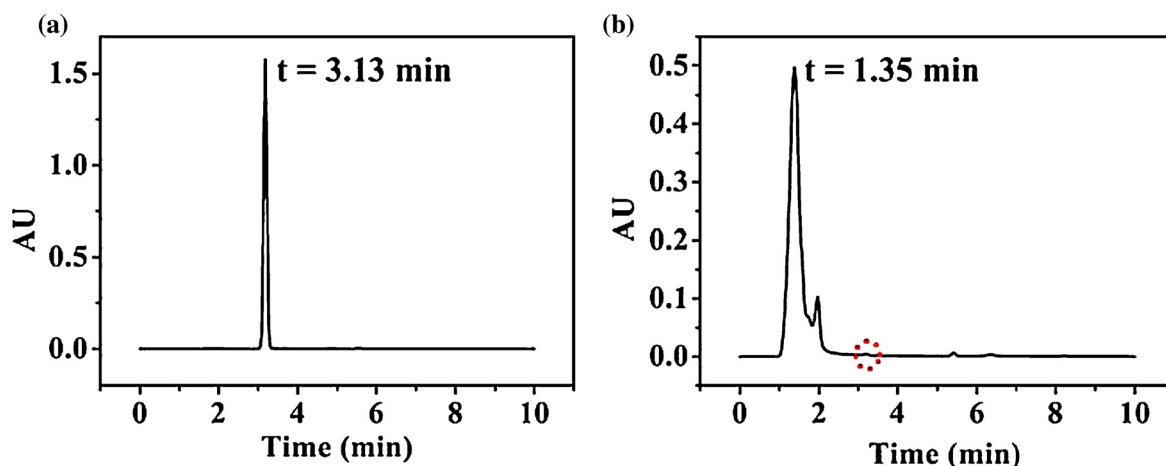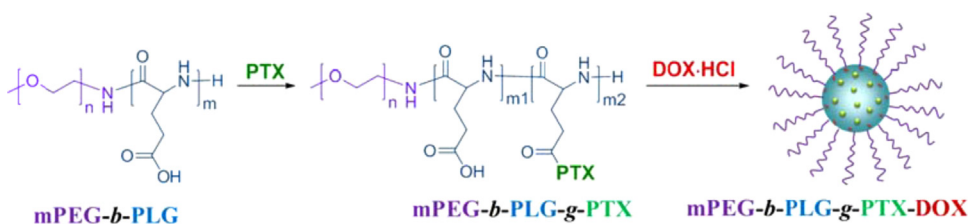

Fig. 2. The HPLC measurement of free PTX (a) and mPEG-*b*-PLG-*g*-PTX (b) dissolved in acetonitrile and water (4:1, v/v).

Scheme 1. The schematic illustration of the process of preparing mPEG-*b*-PLG-*g*-PTX and mPEG-*b*-PLG-*g*-PTX-DOX.

Table 1
Properties of drug loaded nanoparticles.

Nanoparticle	D_h (nm)[a]			Zeta potential (mV)	DLC (wt%)[b]		DLE (wt%)[c]	
	pH 5.4	pH 6.8	pH 7.4		PTX	DOX	PTX	DOX
mPEG-*b*-PLG-*g*-PTX	87.9 ± 2.1	21.8 ± 1.1	22.1 ± 1.1	−36	24.6	–	96	–
mPEG-*b*-PLG-*g*-PTX-DOX	59.4 ± 1.4	66.3 ± 1.3	73.1 ± 1.7	−7	23.0	7.1	–	83

[a] Mean ± standard deviation, determined by DLS.
[b] Drug loading content.
[c] Drug loading efficiency.

of PTX) to peak *b* (—CH$_2$CH$_2$O—, 4H, PEG block), DLC of PTX and PTX grafting ratio in mPEG-*b*-PLG-*g*-PTX were calculated to be 24.6 wt% and 13.2%. HPLC curves of free PTX and mPEG-*b*-PLG-*g*-PTX were showed in Fig. 2. The peak of PTX at 3.13 min disappeared in the spectrum of mPEG-*b*-PLG-*g*-PTX, which indicated free PTX did not exist in the mPEG-*b*-PLG-*g*-PTX. This further confirmed that PTX was grafted on mPEG-*b*-PLG successfully but not loaded into the mPEG-*b*-PLG through hydrophobic interaction.

As shown in Scheme 1, mPEG-*b*-PLG-*g*-PTX-DOX nanoparticles were prepared by the electrostatic and hydrophobic interaction between mPEG-*b*-PLG-*g*-PTX and DOX. The DLC and DLE of DOX were calculated to be 7.1 and 83 wt%, respectively. The hydrodynamic diameter (D_h) of mPEG-*b*-PLG-*g*-PTX and mPEG-*b*-PLG-*g*-PTX-DOX nanoparticles at various pH were shown in Table 1. The D_h of mPEG-*b*-PLG-*g*-PTX at pH 5.4, 6.8 and 7.4 was 87.9 ± 2.1, 21.8 ± 1.1, and 22.1 ± 1.1 nm, respectively. The size of mPEG-*b*-PLG-*g*-PTX at pH 5.4 was signficantly larger, which may be the result from the increased hydrophobicity of glutamic acid residues because of the protonated glutamic acid units in the low pH (Huang et al., 2013b). The D_h of mPEG-*b*-PLG-*g*-PTX-DOX at pH 5.4, 6.8 and 7.4 was 59.4 ± 1.4, 66.3 ± 1.3, and 73.1 ± 1.7 nm, respectively. This indicated that pH condition had only silght influence on the size of mPEG-*b*-PLG-*g*-PTX-DOX nanoparticles. The sizes of both mPEG-*b*-PLG-*g*-PTX and mPEG-*b*-PLG-*g*-PTX-DOX nanoparticles were in the range reported to be retained in the blood circulation system after intravenous administration and to access tumors *via* the leaky vasculature by means of the EPR effect (<400 nm) (Hrkach et al., 2012), which indicated the nanoparticles might passively target to solid tumors. The zeta-potential of mPEG-*b*-PLG-*g*-PTX nanoparticles was −36 mV. After DOX loading, the zeta-potential value changed to −7 mV. This was because the electrostatic interaction between DOX·HCl and negative carbxylate groups reduced the surface charge density of mPEG-*b*-PLG-*g*-PTX-DOX nanoparticles. The slightly low negative surface charge will minimize the undesirable rapid elimination of the mPEG-*b*-PLG-*g*-PTX-DOX nanoparticles from the blood circulation and facilitate their accumulation at the tumor sites by EPR effect (Huang et al., 2013a; Xiao et al., 2011).

3.2. In vitro release of DOX

The release behavior of DOX from mPEG-*b*-PLG-*g*-PTX-DOX nanoparticles was investigated using the dialysis method with PBS at pH 5.4, 6.8 and 7.4, separately. Typical release profiles were shown in Fig. 3. Significantly faster drug release was observed at pH 5.4 and 6.8 than at pH 7.4, which might result from that the protonation of carboxylic groups of glutamic acid units weakened the electrostatic interaction of DOX with carboxylic groups of mPEG-*b*-PLG-*g*-PTX. Considering the pH value in blood, tumor extracellular fluid, and endosome is 7.35–7.45, 6.5–7.2, and 5.0–6.5, respectively (Huang et al., 2013a). The release rate of DOX from the mPEG-*b*-PLG-*g*-PTX-DOX nanoparticles will increase after nanoparticles arrive at tumor tissue and cells; therefore, the mPEG-*b*-PLG-*g*-PTX-DOX nanoparticles would be suitable for tumor intracellular drug delivery.

3.3. Cell uptake study

To investigate the cellular internalization of nanoparticles, intracellular release of DOX, and the influence of DOX-loading on the cellular uptake of mPEG-*b*-PLG-*g*-PTX, the free DOX·HCl, FITC labeled mPEG-*b*-PLG-*g*-PTX, and FITC labeled mPEG-*b*-PLG-*g*-PTX-DOX nanoparticles were incubated with MCF-7cells for 1 and 3 h at 37 °C. The cellular uptake was investigated utilizing confocal laser scanning microscopy. The cellular nuclei of MCF-7cells was selectively stained with DAPI (blue). Red fluorescence imaging was carried out to visualize the released DOX. Green fluorescence imaging was utilized to visualize FITC (Fig. 4). For all of the samples,
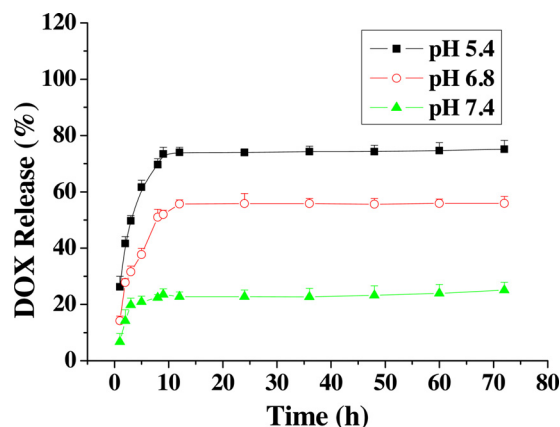

Fig. 3. Time and pH-dependent DOX release profiles of mPEG-*b*-PLG-*g*-PTX-DOX in (A) PBS at pH 5.4, (B) PBS at pH 6.8, (C) PBS at pH 7.4. The data presented are means ± SD (n = 3).

a time dependent cellular accumulation was observed as much higher fluorescent intensity was seen at 3 h than those at 1 h. After 1 h incubation with free DOX·HCl (A), FITC labeled mPEG-*b*-PLG-*g*-PTX (B) or FITC labeled mPEG-*b*-PLG-*g*-PTX-DOX (C) nanoparticles, the DOX fluorescence of A and C was found to be aggregated in the cytosol and nuclei. The FITC fluorescence of B and C was present in the cytosol and nuclear membranes of MCF-7cells but not nuclei. When the incubation period was increased to 3 h, DOX of C had mostly released into the nuclei region of cells. The FITC fluorescence

of B and C increased in the cytosol and nuclear membranes but was not distributed in the nuclei. This implied that more nanovehicles and mPEG-*b*-PLG-*g*-PTX-DOX nanoparticles entered into the cells as the culture time prolonged. The FITC accumulation in MCF-7cells for mPEG-*b*-PLG-*g*-PTX-DOX nanoparticles was a bit higher than that for the mPEG-*b*-PLG-*g*-PTX nanoparticles. This may be due to the decreased negative surface charge of mPEG-*b*-PLG-*g*-PTX-DOX as compared with mPEG-*b*-PLG-*g*-PTX (Table 1). Because the cell membrane is negative-charged, nanoparticles with lower negative
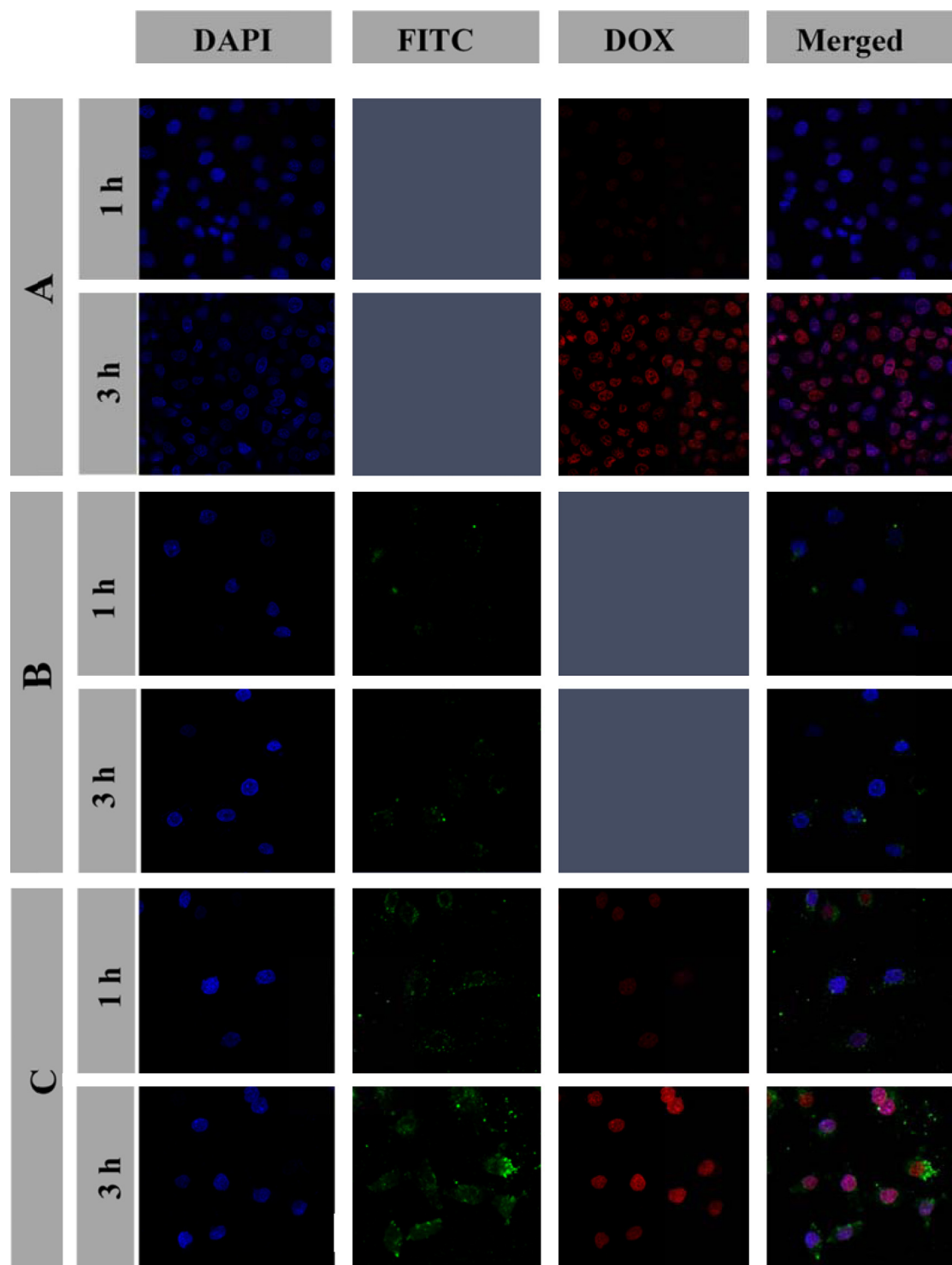

Fig. 4. Confocal laser scanning microscopic observation of MCF-7cells after incubation with free DOX·HCl (A), FITC labeled mPEG-*b*-PLG-*g*-PTX (B), FITC labeled mPEG-*b*-PLG-*g*-PTX-DOX (C) for 1 h and 3 h. (For interpretation of the references to color in this figure legend, the reader is referred to the web version of this article.)
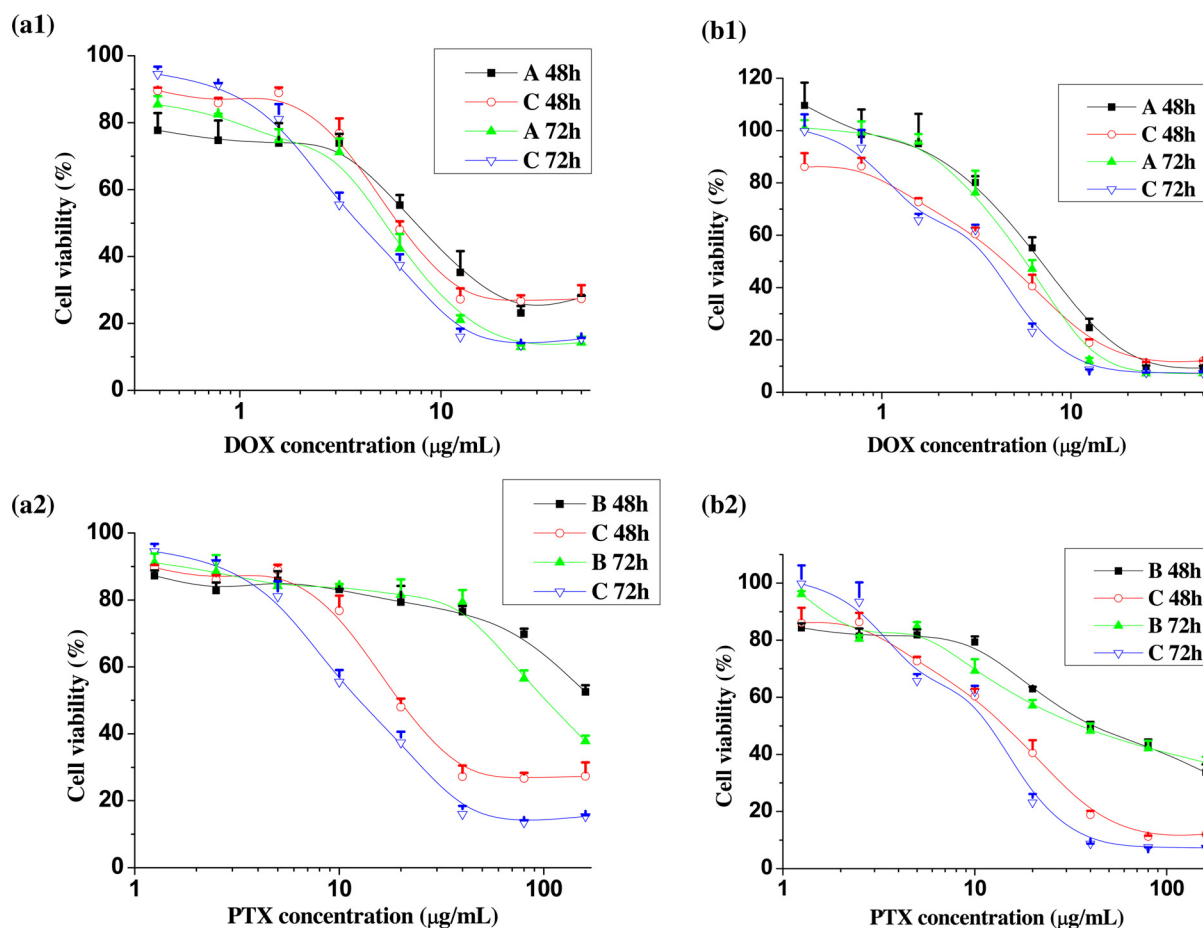
Fig. 5. *In vitro* cytotoxicities of (A) free DOX·HCl, (B) mPEG-*b*-PLG-*g*-PTX, and (C) mPEG-*b*-PLG-*g*-PTX-DOX to A549 (a_1, a_2) and MCF-7 (b_1, b_2) cells ($n = 3$, mean ± SD).

surface charge density are familiar for cell endocytosis (Miller et al., 1998).

3.4. In vitro cytotoxicity assay

The cytotoxicities of free DOX·HCl, mPEG-*b*-PLG-*g*-PTX, mPEG-*b*-PLG-*g*-PTX-DOX were evaluated against MCF-7 and A549cells using MTT assays. As shown in Fig. 5, all the samples showed dose and time dependent cell proliferation inhibition behavior. Loaded-DOX dominated the cell proliferation inhibition since the IC_{50} of loaded-DOX was much lower than that of grafted-PTX. The inhibition concentrations are summarized in Table 2, with IC_x

means drug concentration when the inhibition rate was $x\%$. For A549cells at 48 h, the IC_{35} of mPEG-*b*-PLG-*g*-PTX was 94.7 μg/mL, the IC_{50} and IC_{60} of mPEG-*b*-PLG-*g*-PTX were above 160 μg/mL. In contrast, the IC_{35}, IC_{50} and IC_{60} at 48 h on the PTX basis of mPEG-*b*-PLG-*g*-PTX-DOX to A549cells decreased to 13.1, 19.4, and 26.7 μg/mL, respectively. Similar phenomena could be observed for A549cells at 72 h, and MCF-7cells at 48 and 72 h. These may be because the cell proliferation inhibition was dominated by loaded-DOX in the co-delivery system mPEG-*b*-PLG-*g*-PTX-DOX. Therefore, the mPEG-*b*-PLG-*g*-PTX-DOX showed higher cytotoxicity than mPEG-*b*-PLG-*g*-PTX and comparable cytotoxicity with free DOX·HCl. Because the PLG backbone could be cleaved by

Table 2
IC_x values for free DOX·HCl, mPEG-*b*-PLG-*g*-PTX, and mPEG-*b*-PLG-*g*-PTX-DOX, combination index (CI) of PTX and CDDP in mPEG-*b*-PLG-*g*-PTX-DOX.

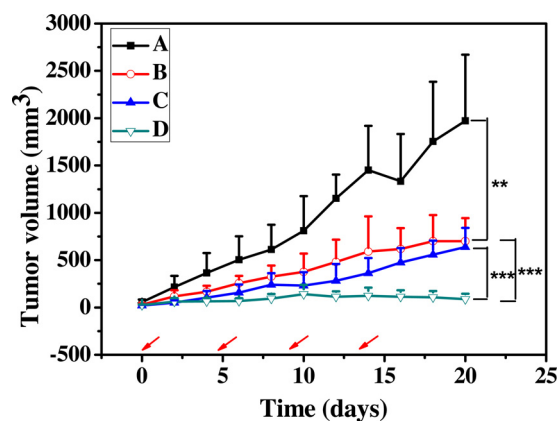|			Free DOX·HCl	mPEG-*b*-PLG-*g*-PTX	mPEG-*b*-PLG-*g*-PTX-DOX		
			DOX/μg/mL	PTX/μg/mL	DOX/μg/mL	PTX/μg/mL	CI
IC_{35}	A549	48 h	4.3	94.7	4.1	13.1	1.09
		72 h	3.4	61.7	2.4	7.7	0.83
	MCF-7	48 h	4.7	18.6	2.4	7.7	0.92
		72 h	4.0	13.0	2.0	6.4	0.99
IC_{50}	A549	48 h	7.4	–	6.0	19.4	–
		72 h	5.2	102.2	3.9	12.5	0.87
	MCF-7	48 h	6.9	41.7	4.4	14.2	0.98
		72 h	5.8	34.7	3.7	11.9	0.98
IC_{60}	A549	48 h	10.8	–	8.3	26.7	–
		72 h	6.9	149.0	5.5	17.9	0.92
	MCF-7	48 h	8.9	99.4	6.3	20.0	0.91
		72 h	7.1	111.5	4.6	14.8	0.78

Fig. 6. *In vivo* antitumor efficacies of various samples in Balb-c/nude mice bearing orthotopic human breast tumors (MCF-7). Tumor sizes of the mice as a function of time. The mice were treated on days 0, 4, 8 and 12 with (A) PBS, (B) free DOX·HCl, (C) mPEG-*b*-PLG-*g*-PTX, (D) mPEG-*b*-PLG-*g*-PTX-DOX. $n = 5$ or 6, mean ± SD, *$p<0.05$, **$p<0.01$, ***$p<0.001$. The average initial volume of the tumor of group A, B, C, and D was 49, 30, 25, and 28 mm^3, respectively.

proteolysis to form both mono- and diglutamyl-paclitaxel intermediate metabolites and was followed by hydrolysis to yield free paclitaxel (Shaffer et al., 2007; Singer et al., 2003), it was reasonable that the mPEG-*b*-PLG-*g*-PTX showed some cytotoxicity to cancer cells such as A549 and MCF-7. The synergistic effect of DOX and PTX in the mPEG-*b*-PLG-*g*-PTX-DOX was evaluated from a combination index (CI) analysis. Values of CI > 1 represented antagonism, CI = 1 represented additive, and CI < 1 represented synergism. As shown in Table 2, the values of CI of PTX and CDDP in mPEG-*b*-PLG-*g*-PTX-DOX were slightly less than 1 in most cases except IC$_{35}$ for A549 at 48 h. This indicated there was slight synergistic effect in the PTX and DOX co-delivery system of mPEG-*b*-PLG-*g*-PTX-DOX.

3.5. In vivo *antitumor efficiency*

In order to further examine the dual-drug co-delivery system of mPEG-*b*-PLG-*g*-PTX-DOX, the *in vivo* antitumor efficiency was investigated on Balb-c/nude mice bearing orthotopic human breast tumors (MCF-7). PBS, free DOX·HCl, mPEG-*b*-PLG-*g*-PTX, and mPEG-*b*-PLG-*g*-PTX-DOX were injected *via* tail vein, respectively. As shown in Fig. 6, tumor volume of PBS treatment group increased rapidly, while all the chemotherapy groups were effective in retarding tumor growth. The mPEG-*b*-PLG-*g*-PTX-DOX showed significantly higher tumor suppression rate (TSR% = 95.5%) than the corresponding free DOX·HCl and mPEG-*b*-PLG-*g*-PTX groups (TSR% = 59.7% for free DOX·HCl group and 67.7% for mPEG-*b*-PLG-*g*-PTX group). More importantly, the dual-drug loaded nanoparticles mPEG-*b*-PLG-*g*-PTX-DOX showed continued tumor regression and no obvious recurrence in 8 days after the last drug administration. This indicated that the dual co-delivery strategy had the potential to enhance the efficacy of anticancer drugs.

4. Conclusion

We present here a doxorubicin and paclitaxel combination strategy based on polypeptide nanoparticles for enhanced chemotherapy efficacy. PTX and DOX were encapsulated into mPEG-*b*-PLG *via* chemical conjugation and electrostatic complexation, respectively. The resultant dual-drug loaded nanoparticles mPEG-*b*-PLG-*g*-PTX-DOX showed some synergistic effects in inhibition of the proliferation of A549 and MCF-7 human cancer cells. *In vivo* study demonstrated that the polypeptide-based combination of DOX and PTX exhibited improved inhibition toward MCF-7 tumor growth

than the related single anticancer agents such as free DOX·HCl and mPEG-*b*-PLG-*g*-PTX. The tumor suppression rate for the groups of mPEG-*b*-PLG-*g*-PTX-DOX, free DOX·HCl and mPEG-*b*-PLG-*g*-PTX is 95.5%, 59.7%, and 67.7%, respectively. Therefore, the mPEG-*b*-PLG-*g*-PTX-DOX is a potential dual-drug co-delivery system with synergistic effect for cancer chemotherapy.

Acknowledgments

References

Blanco, E., Hsiao, A., Mann, A.P., Landry, M.G., Meric-Bernstam, F., Ferrari, M., 2011. Nanomedicine in cancer therapy: innovative trends and prospects. Cancer Sci. 102, 1247–1252.

Boulikas, T., Vougiouka, M., 2004. Recent clinical trials using cisplatin, carboplatin and their combination chemotherapy drugs (review). Oncol. Rep. 11, 559–595.

Chen, F., Dong, D., Fu, Y., Zheng, Y., Liu, S., Chang, M., Jing, X., 2012. Anti-tumor activity of biodegradable polymer-paclitaxel conjugated micelle against mice U14cervical cancers. Chem. Res. Chin. Univ. 28, 656–661.

Choe, U.-J., Sun, V., Tan, J.-K., Kamei, D., 2012. Self-assembled polypeptide and polypeptide hybrid vesicles: from synthesis to application. In: Deming, T. (Ed.), Peptide-based Materials. Springer, Berlin, Heidelberg, pp. 117–134.

Chou, T.C., 2006. Theoretical basis, experimental design, and computerized simulation of synergism and antagonism in drug combination studies. Pharmacol. Rev. 58, 621–681.

Deming, T.J., 2007. Synthetic polypeptides for biomedical applications. Prog. Polym. Sci. 32, 858–875.

Deng, C., Jiang, Y., Cheng, R., Meng, F., Zhong, Z., 2012. Biodegradable polymeric micelles for targeted and controlled anticancer drug delivery: promises, progress and prospects. Nano Today 7, 467–480.

Duncan, R., 2006. Polymer conjugates as anticancer nanomedicines. Nat. Rev. Cancer 6, 688–701.

Gehl, J., Boesgaard, M., Paaske, T., Jensen, B.V., Dombernowsky, P., 1996. Combined doxorubicin and paclitaxel in advanced breast cancer: effective and cardiotoxic. Ann. Oncol. 7, 687–693.

Greenberg, S., Rugo, H.S., 2010. Challenging clinical scenarios: treatment of patients with triple-negative or basal-like metastatic breast cancer. Clin. Breast Cancer 10 2, S20–S29.

Hrkach, J., Von Hoff, D., Ali, M.M., Andrianova, E., Auer, J., Campbell, T., De Witt, D., Figa, M., Figueiredo, M., Horhota, A., Low, S., McDonnell, K., Peeke, E., Retnarajan, B., Sabnis, A., Schnipper, E., Song, J.J., Song, Y.H., Summa, J., Tompsett, D., Troiano, G., Van Geen Hoven, T., Wright, J., LoRusso, P., Kantoff, P.W., Bander, N.H., Sweeney, C., Farokhzad, O.C., Langer, R., Zale, S., 2012. Preclinical development and clinical translation of a PSMA-targeted docetaxel nanoparticle with a differentiated pharmacological profile. Sci. Transl. Med. 4, 128139.

Huang, Y., Tang, Z., Zhang, X., Yu, H., Sun, H., Pang, X., Chen, X., 2013a. pH-triggered charge-reversal polypeptide nanoparticles for cisplatin delivery: preparation and in vitro evaluation. Biomacromolecules 14, 2023–2032.

Huang, Y., Tang, Z.H., Zhang, X.F., Yu, H.Y., Sun, H., Pang, X., Chen, X.S., 2013b. Ph-triggered charge-reversal polypeptide nanoparticles for cisplatin delivery: preparation and in vitro evaluation. Biomacromolecules 14, 2023–2032.

Huynh, N.T., Passirani, C., Saulnier, P., Benoit, J.P., 2009. Lipid nanocapsules: a new platform for nanomedicine. Int. J. Pharm. 379, 201–209.

Kieler-Ferguson, H.M., Fréchet, J.M.J., Szoka Jr, F.C., 2013. Clinical developments of chemotherapeutic nanomedicines: polymers and liposomes for delivery of camptothecins and platinum (II) drugs. Wiley Interdiscip. Rev. Nanomed. Nanobiotechnol. 5, 130–138.

Langer, C.J., O'Byrne, K.J., Socinski, M.A., Mikhailov, S.M., Lesniewski-Kmak, K., Smakal, M., Ciuleanu, T.E., Orlov, S.V., Dediu, M., Heigener, D., 2008. Phase III trial comparing paclitaxel poliglumex (CT-2103, PPX) in combination with carboplatin versus standard paclitaxel and carboplatin in the treatment of PS 2 patients with chemotherapy-naive advanced non-small cell lung cancer. J. Thoracic Oncol. 3, 623–630.

Lee, A.L.Z., Wang, Y., Cheng, H.Y., Pervaiz, S., Yang, Y.Y., 2009. The co-delivery of paclitaxel and Herceptin using cationic micellar nanoparticles. Biomaterials 30, 919–927.

Lei, Y., Lai, Y., Li, Y., Li, S., Cheng, G., Li, D., Li, H., He, B., Gu, Z., 2013. Anticancer drug delivery of PEG based micelles with small lipophilic moieties. Int. J. Pharm. 453, 579–586.

Li, D., Ding, J.X., Tang, Z.H., Sun, H., Zhuang, X.L., Xu, J.Z., Chen, X.S., 2012. In vitro evaluation of anticancer nanomedicines based on doxorubicin and amphiphilic Y-shaped copolymers. Int. J. Nanomed. 7, 2687–2697.

Li, M., Lv, S., Tang, Z., Song, W., Yu, H., Sun, H., Liu, H., Chen, X., 2013a. Polypeptide/doxorubicin hydrochloride polymersomes prepared through organic solvent-free technique as a smart drug delivery platform. Macromol. Biosci. 13, 1150–1162.

Li, M., Song, W., Tang, Z., Lv, S., Lin, L., Sun, H., Li, Q., Yang, Y., Hong, H., Chen, X., 2013b. Nanoscaled poly(l-glutamic acid)/doxorubicin-amphiphile complex as ph-responsive drug delivery system for effective treatment of nonsmall cell lung cancer. Acs. Appl. Mater. Inter. 5, 1781–1792.

Li, Y., Xiao, K., Zhu, W., Deng, W., Lam, K.S., 2014. Stimuli-responsive cross-linked micelles for on-demand drug delivery against cancers. Adv. Drug Deliv. Rev. 66, 58–73.

Liu, J., Kopečková, P., Pan, H., Sima, M., Bühler, P., Wolf, P., Elsässer-Beile, U., Kopeček, J., 2012. Prostate-cancer-targeted n-(2-hydroxypropyl)methacrylamide copolymer/docetaxel conjugates. Macromol. Biosci. 12, 412–422.

Lv, S., Li, M., Tang, Z., Song, W., Sun, H., Liu, H., Chen, X., 2013. Doxorubicin-loaded amphiphilic polypeptide-based nanoparticles as an efficient drug delivery system for cancer therapy. Acta Biomater. 9, 9330–9342.

Matsumura, Y., 2008. Poly (amino acid) micelle nanocarriers in preclinical and clinical studies. Adv. Drug Deliv. Rev. 60, 899–914.

Miller, C.R., Bondurant, B., McLean, S.D., McGovern, K.A., O'Brien, D.F., 1998. Liposome–cell interactions in vitro: effect of liposome surface charge on the binding and endocytosis of conventional and sterically stabilized liposomes. Biochemistry 12875–12883.

Pan, H., Sima, M., Yang, J., Kopeček, J., 2013. Synthesis of long-circulating, backbone degradable hpma copolymer–doxorubicin conjugates and evaluation of molecular-weight-dependent antitumor efficacy. Macromol. Biosci. 13, 155–160.

Park, J.H., Lee, S., Kim, J.-H., Park, K., Kim, K., Kwon, I.C., 2008. Polymeric nanomedicine for cancer therapy. Prog. Polym. Sci. 33, 113–137.

Reddy, L.H., Bazile, D., 2013. Drug delivery design for intravenous route with integrated physicochemistry, pharmacokinetics and pharmacodynamics: illustration with the case of taxane therapeutics. Adv. Drug Deliv. Rev. .

Rowinsky, E.K., Eisenhauer, E.A., Chaudhry, V., Arbuck, S.G., Donehower, R.C., 1993. Clinical toxicities encountered with paclitaxel (Taxol). Semin. Oncol. 20, 1–15.

Shaffer, S.A., Baker-Lee, C., Kennedy, J., Lai, M.S., de Vries, P., Buhler, K., Singer, J.W., 2007. In vitro and in vivo metabolism of paclitaxel poliglumex: identification of metabolites and active proteases. Cancer Chemoth. Pharm. 59, 537–548.

Shen, J., Song, G., An, M., Li, X., Wu, N., Ruan, K., Hu, J., Hu, R., 2014. The use of hollow mesoporous silica nanospheres to encapsulate bortezomib and improve efficacy for non-small cell lung cancer therapy. Biomaterials 35, 316–326.

Siegel, R., Naishadham, D., Jemal, A., 2013. Cancer statistics. CA: Cancer J. Clin. 63, 11–30.

Singer, J.W., Baker, B., De Vries, P., Kumar, A., Shaffer, S., Vawter, E., Bolton, M., Garzone, P., 2003. Poly-(L)-glutamic acid-paclitaxel (CT-2103) [XYOTAX (TM)], a biodegradable polymeric drug conjugate – characterization, preclinical pharmacology, and preliminary clinical data. Adv. Exp. Med. Biol. 519, 81–99.

Song, W., Li, M., Tang, Z., Li, Q., Yang, Y., Liu, H., Duan, T., Hong, H., Chen, X., 2012a. Methoxypoly(ethylene glycol)-block-poly(L-glutamic acid)-loaded cisplatin and a combination with iRGD for the treatment of non-small-cell lung cancers. Macromol. Biosci. 12, 1514–1523.

Song, W., Tang, Z., Li, M., Lv, S., Sun, H., Deng, M., Liu, H., Chen, X., 2014. Polypeptide-based combination of paclitaxel and cisplatin for enhanced chemotherapy efficacy and reduced side-effects. Acta Biomater. 10, 1392–1402.

Song, W., Tang, Z., Li, M., Lv, S., Yu, H., Ma, L., Zhuang, X., Huang, Y., Chen, X., 2012b. Tunable ph-sensitive poly(β-amino ester)s synthesized from primary amines and diacrylates for intracellular drug delivery. Macromol. Biosci. 12, 1375–1383.

Song, W.T., Li, M.Q., Tang, Z.H., Li, Q.S., Yang, Y., Liu, H.Y., Duan, T.C., Hong, H., Chen, X.S., 2012c. Methoxypoly(ethylene glycol)-block-poly(L-glutamic acid)-loaded cisplatin and a combination with iRGD for the treatment of non-small-cell lung cancers. Macromol. Biosci. 12, 1514–1523.

Wang, M.D., Shin, D.M., Simons, J.W., Nie, S., 2007. Nanotechnology for targeted cancer therapy. Expert Rev. Anticancer Ther. 7, 833–837.

Weiss, R.B., 1992. The anthracyclines: will we ever find a better doxorubicin? Semin. Oncol. 19, 670–686.

Xiang, B., Dong, D.-W., Shi, N.-Q., Gao, W., Yang, Z.-Z., Cui, Y., Cao, D.-Y., Qi, X.-R., 2013. PSA-responsive and PSMA-mediated multifunctional liposomes for targeted therapy of prostate cancer. Biomaterials 34, 6976–6991.

Xiao, H.H., Li, W.L., Qi, R.G., Yan, L.S., Wang, R., Liu, S., Zheng, Y.H., Xie, Z.G., Huang, Y. B., Jing, X.B., 2012. Co-delivery of daunomycin and oxaliplatin by biodegradable polymers for safer and more efficacious combination therapy. J. Control Release 163, 304–314.

Xiao, K., Li, Y.P., Luo, J.T., Lee, J.S., Xiao, W.W., Gonik, A.M., Agarwal, R.G., Lam, K.S., 2011. The effect of surface charge on in vivo biodistribution of PEG-oligocholic acid based micellar nanoparticles. Biomaterials 32, 3435–3446.

Xu, J.P., Chen, W.D., Ji, J., Shen, J.C., 2007. Novel biomimetic polymeric micelles for drug delivery. Chem. J. Chin. U 28, 394–396.

Zhang, Z., Mei, L., Feng, S.-S., 2013. Paclitaxel drug delivery systems. Expert Opin. Drug Deliv. 10, 325–340.

Zhong, Y., Yang, W., Sun, H., Cheng, R., Meng, F., Deng, C., Zhong, Z., 2013. Ligand-directed reduction-sensitive shell-sheddable biodegradable micelles actively deliver doxorubicin into the nuclei of target cancer cells. Biomacromolecules 14, 3723–3730.